JACS
JOURNAL OF THE AMERICAN CHEMICAL SOCIETY

ARTICLE

pubs.acs.org/JACS

Localized Electron Transfer and the Effect of Tunneling on the Rates of $Ru(bpy)_3^{2+}$ Oxidation and Reduction As Measured by Scanning Electrochemical Microscopy

Mei Shen and Allen J. Bard*

Center for Electrochemistry, Department of Chemistry and Biochemistry, University of Texas at Austin, 1 University Station, A5300, Austin, Texas 78712-0165, United States

ABSTRACT: The kinetics of tris(2,2′-bipyridine)ruthenium(II) (Ru(bpy)) oxidation and reduction in acetonitrile were investigated by steady-state voltammetry using scanning electrochemical microscopy (SECM). The SECM setup was placed inside a drybox for carrying out experiments in an anhydrous atmosphere and in the absence of oxygen. The standard rate constant, $k°$, for Ru(bpy) oxidation at a Pt electrode (radius, a = 5 μm) was 0.7 ± 0.1 cm/s, which is smaller than $k°$ for Ru(bpy) reduction measured under the same conditions (≥3 cm/s). This is attributed to the 2,2′-bipyridine ligands having an electron-transfer (ET) blocking effect on the oxidation of the ruthenium(II) center, as opposed to the reduction, which involves ET to the exposed ligands. Thus, tunneling effects may be important in considering the ET in this molecule.

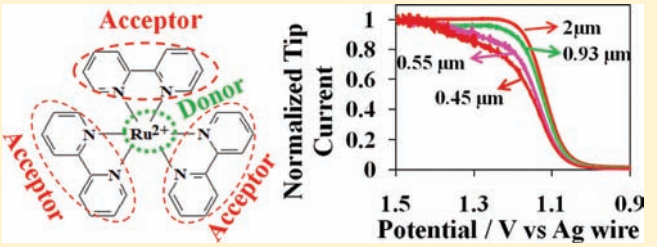

INTRODUCTION

In considering heterogeneous electron transfer (ET), molecules in which different moieties are not conjugated with one another often show electrochemistry in which each moiety behaves independently and resembles that of that portion alone. Such localized ET is seen for example in some oligomers and polymers, e.g., poly(vinylferrocene), where each monomer unit behaves independently. Many donor−acceptor (D−A) molecules, with general structures that involve the linking of a donor group to an acceptor group, D∼(L)∼A (where L represents the linker), also can show localized ET to A and D. For example, in the dithienylbenzothiadiazole-based molecule **1b** (4,7-bis(4-(4-*sec*-butoxyphenyl)-5-(3,5-di(1-naphthyl)phenyl)thiophen-2-yl)-2,1,3-benzothiadiazole) shown in Scheme 1, the benzothiadiazole (A) and the two thienyl moieties (D) are weakly coupled, even though they are directly linked, probably because of steric interactions.[1] In this D−A molecule, the heterogeneous ET rate constants, $k°$, for the oxidation of D and the reduction of A were different. This was ascribed to differences in the ET distances involved, where the A, with the smaller $k°$, was blocked by the bulky D groups from close approach to the electrode surface, while the D groups themselves were accessible. Thus, differences in tunneling, rather than differences in reorganization energies, were taken as the main factor to explain the results.

Tunneling effects can be important factors influencing the rates of ET and are described by eq 1, where k_{ET} is the effective rate of electron transfer, $k°_{ET}$ is the rate of electron transfer in the absence of barrier effects, β is the tunneling constant, and x is the tunneling distance:

$$k_{ET} = k°_{ET}\, e^{-\beta x} \quad (1)$$

Tunneling effects on the rates of electrochemical processes have been studied by making use of the exponential dependence on distance shown in eq 1; this is accomplished generally by separating the electrode surface from the electroactive species by using a spacer, e.g., a self-assembled monolayer, or by connecting the electroactive species on the end of a linker.[2−5]

An advantage of studying tunneling effects in D−A molecules is that comparison of oxidation and reduction rate constants can be made on the same molecule under identical electrode and solution conditions, thus minimizing impacts of electrode surface blockage, uncompensated resistance effects, and other variables that might affect the measured value of the heterogeneous rate constant. The extensively studied molecule tris(2,2′-bipyridine)-ruthenium(II) (Ru(bpy)) (see Scheme 1) is in fact also a D−A complex that consists of an oxidizable ruthenium center (D) coordinated by three 2,2′-bipyridine ligands (A) that can be reduced in MeCN solution.[6] Surprisingly, the rate constants for the reduction and oxidation of Ru(bpy) at an electrode in MeCN have not been measured previously, perhaps because these rates are high. Sun and Mirkin[7] tried to measure the rate constants for Ru(bpy) oxidation in aqueous and organic solvents at a nanometer-size ultramicroelectrode (UME), but a decrease in the limiting current, probably because of impurities, prevented quantitative studies. We show here that scanning electrochemical microscopy (SECM) can be employed to measure the relative rates and propose that the difference in the rate constants can arise from tunneling effects.

SECM has been used to study the kinetics of heterogeneous ET with high accuracy.[7−11] In SECM, a micrometer-size UME is

Received: July 1, 2011
Published: August 15, 2011

Scheme 1

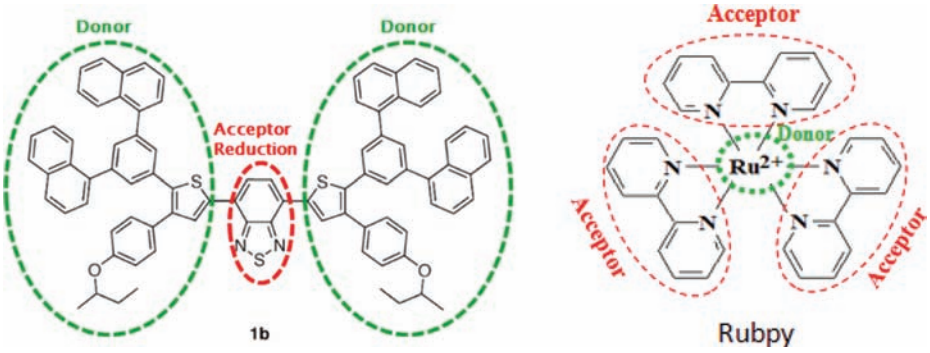

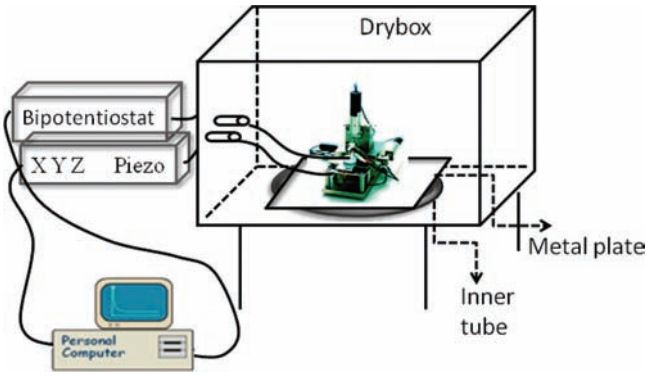

Figure 1. Diagram of SECM inside a drybox.

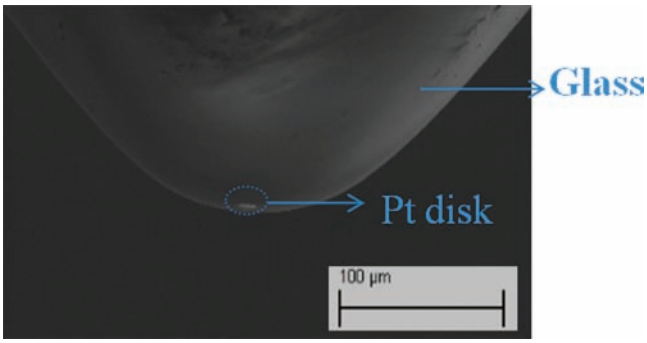

Figure 2. SEM picture of UME tip tilted at 15°. The brighter spot at the end of the tip is the 10 μm diameter Pt, and the remainder is glass.

approached to a substrate electrode held at a potential where the product of the half-reaction at the UME tip regenerates the starting material. The rate of ET of a solution species at the tip can be measured by observing the feedback current, detected as a function of the distance, d, between the tip and substrate, and noting deviations from the behavior for a diffusion-controlled reaction.[12] Because the tip current is measured at steady state and small currents (~nA) are detected, fast kinetics can be measured without having to deal with electrode capacitive effects and uncompensated resistance, which can be especially important in nonaqueous solvents. However, to measure large heterogeneous rate constants, the mass-transfer rate, proportional to D/d, where D is the diffusion coefficient of the molecule under study, must be large compared with $k°$, so the tip−substrate distance must be small compared with the tip radius, a.[13]

EXPERIMENTAL SECTION

Chemicals. Anhydrous acetonitrile (MeCN) was obtained from Aldrich (St. Louis, MO) and transferred directly into an argon atmosphere drybox (MBraun Inc., Stratham, NH) without further purification. Electrochemical-grade tetra-*n*-butylammonium hexafluorophosphate ($TBAPF_6$) was obtained from Fluka and used as received. Tris(2,2′-bipyridine)ruthenium(II) perchlorate was obtained from GFS Chemicals, Inc. (Powell, OH).

Setup. All SECM and other electrochemical measurements were carried out with a CHI 920C SECM station bipotentiostat (CH Instruments, Austin, TX). The SECM scanning head and cell were placed inside the drybox and connected to the controller outside the glovebox via a feed-through. This was necessary to avoid contamination of the solution with water and oxygen. A partially inflated inner tube was placed beneath the SECM to minimize vibrations from the glovebox blower, and a metal plate was placed on top of the tire as a stand support. A diagram of the setup is shown is Figure 1.

Electrodes. Platinum (99.99%) 10 μm diameter wire from Goodfellow (Devon, PA) was used to fabricate the SECM electrodes by procedures described elsewhere.[13,14] The glass surrounding the tip was made as small as possible by careful polishing, holding the tip at an angle with respect to the polishing disk. Making such a tip and careful alignment with respect to the substrate were necessary to obtain the very small d/a values required in the measurement. Details about the tip construction and simulations of the tip behavior with geometric variations will be published elsewhere.[15] A Zeiss Supra 40 VP scanning electron microscope (SEM) was used to check the tip geometry, where the tip was initially placed flat (horizontal) and then tilted to different angles to find the optimum one (tilted at 15°) to best characterize the tip end (Figure 2).

The substrate electrode was a Pt disk (2 mm diameter, CH Instruments) sealed in Teflon. The tip and substrate electrodes were polished prior to use with alumina paste (0.3 and 0.05 μm) on microcloth pads (Buehler, Lake Bluff, IL) and subsequently sonicated in Milli-Q deionized water and then in ethanol. The substrate electrode was polished to a mirror finish. The measurement was done in a Teflon cell. A Pt wire (0.5 mm diameter) was used as a counter electrode, and a Ag wire (1 mm in diameter) was used as a quasi-reference electrode. The thermodynamic potential of ferrocene in MeCN vs this Ag reference electrode is 0.356 V. The counter and reference electrodes were cleaned by rinsing and sonicating in acetone, water, and ethanol. Finally, all the electrodes were rinsed with acetone, dried in an oven, and transferred into a glovebox. To make the measurements, very careful alignment of the tip

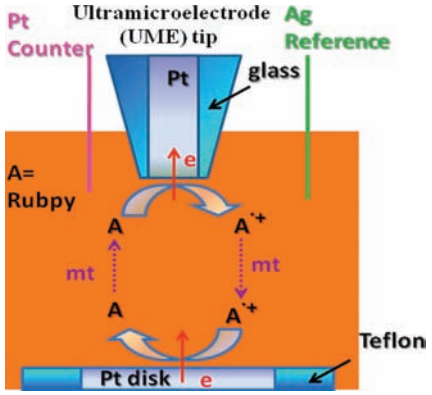

Figure 3. Electrodes and cell configuration.

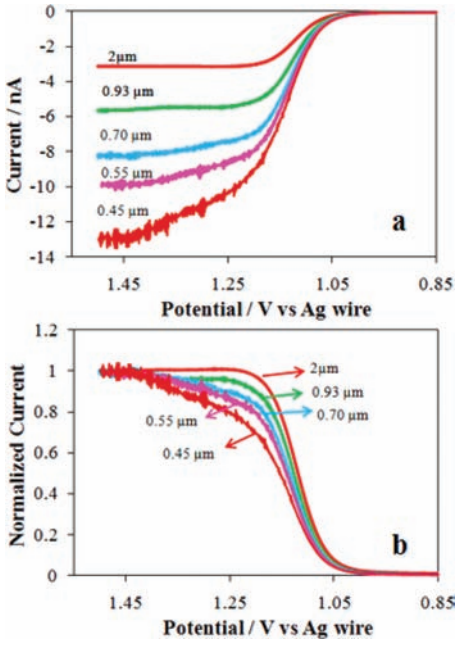

Figure 4. (a) Tip steady-state voltammograms and (b) normalized ($i_T/i_{T,max}$) tip steady-state voltammograms of 0.38 mM Ru(bpy) in MeCN with 0.1 M $TBAPF_6$ as supporting electrolyte at a 5 μm radius Pt tip inside a glovebox; $i_{T,\infty}$= 1.3 nA. The distances, d, between the tip and the substrate are indicated. Scan rate = 0.001 V/s.

and substrate and imaging to find the highest point on the substrate were required, as described in detail elsewhere.[15] The electrodes and cell configuration is shown in Figure 3.

RESULTS AND DISCUSSION

SECM Approach and Heterogeneous Oxidation Kinetics. The kinetics of Ru(bpy) oxidation and reduction at the tip were obtained by a previously described SECM technique in which the tip voltammograms obtained under positive feedback conditions at different tip−substrate distances are fit to a model assuming Butler−Volmer kinetics.[10,16−18] Figure 4a shows tip voltammograms obtained at different d values for the oxidation of the 2+ to 3+ form, while holding the substrate potential where the reaction is diffusion controlled at 0.4 V vs Ag wire. We did not find any change of the current with time, perhaps because our experiments were carried out inside a glovebox. The results show that a higher current was generated when the tip was closer to the substrate, as expected from feedback theory. Note that in this experiment, the a = 5 μm tip could approach to 0.45 μm. Figure 4b presents the normalized voltammograms derived from Figure 4a, where the tip current was normalized with respect to the maximum current, $i_{T,max}$ (the steady-state limiting current), in the voltammograms in Figure 4a. As shown in Figure 4b, the voltammograms become more and more drawn out with decreasing d. Ru(bpy) oxidation shows a diffusion-controlled (nernstian) voltammogram at large d, but as the mass-transfer coefficient is increased with decreasing d, the kinetics of ET make a greater contribution, and kinetic information can be extracted.

The kinetic parameters for the oxidation were obtained through the use of eqs 2−5 (assuming uniform accessibility of the tip surface, i.e., a uniform surface concentration of the electroactive species):[13,16]

$$I_T(E,L) = \frac{0.68 + 0.78377/L + 0.3315\, e^{-1.0672/L}}{\theta + 1/k} \quad (2)$$

$$\theta = 1 + \frac{D_0}{D_R} e^{nf(E - E^{o'})} \quad (3)$$

$$k = \frac{k^{\circ}\, e^{-\alpha nf(E - E^{o'})}}{m_o} \quad (4)$$

$$m_o = \frac{4D_0}{\pi a}\left(0.68 + \frac{0.78377}{L} + 0.3315\, e^{-1.0672/L}\right) \quad (5)$$

where κ is the kinetic parameter and m_o is the effective mass-transfer coefficient. The standard rate constant k° and the transfer coefficient α can be measured in terms of known quantities such as distance d (where $L = d/a$), potential E, standard potential of reaction E°, and steady-state tip current at infinite distance $i_{T,\infty}$. The experimental tip current can be treated with the relation $i_T = I_T(E,L)i_{T,\infty}$.[19] Figure 5 shows the fit obtained for the experimental scans at different distances, and Table 1 summarizes the electrochemical parameters obtained for a series of experiments. The diffusion coefficient (D) of 1.76 × 10^{-5} cm^2/s for Ru(bpy) in MeCN, calculated from the tip steady-state cyclic voltammogram (CV) and used for the calculations, is very close to the D value reported in the literature (e.g., D = 1.8 × 10^{-5} cm^2/s).[20] The average standard reaction rate constant, k°, and transfer coefficient, α, for the oxidation of Ru(bpy) are 0.7 ± 0.1 cm/s and 0.28 ± 0.03, respectively. These results were checked and agreed with those obtained from the quartile potential approach (for a uniformly accessible electrode)[9] (where $E_{1/4}$, $E_{1/2}$, and $E_{3/4}$ are the potentials at which the tip current is one-fourth, one-half, and three-fourths of the diffusion-limiting current). The dimensionless parameter $k^{\circ}/(D/d)$ is also listed in Table 1; the values are <5, as required to obtain kinetic information.

Heterogeneous Reduction Kinetics. The rate constants for Ru(bpy) reduction were obtained by the same approach under identical experimental conditions by examining the negative potential region. Figure 6a,b (pink dotted curves) shows the experimental steady-state voltammograms for Ru(bpy) oxidation and reduction, respectively. The two voltammograms were measured at the same distance. The black dotted curves in Figure 6a,b are the simulated results using the same diffusion coefficient and tip−substrate separation distance. The expected limiting current

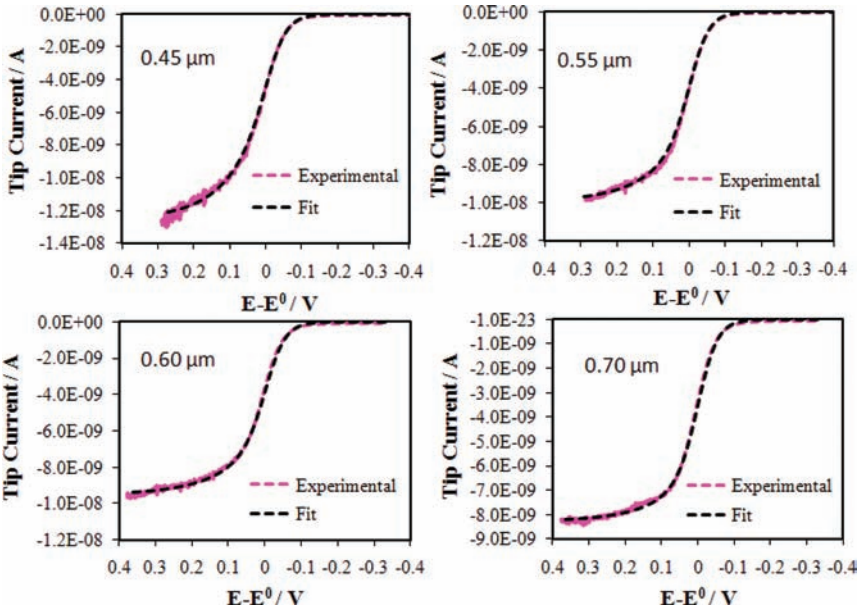

Figure 5. Determination of tip kinetic parameters for Ru(bpy) oxidation with tip−substrate distance shown. The solution contained 0.38 mM Ru(bpy) in MeCN with 0.1 M $TBAPF_6$ as supporting electrolyte. The obtained parameters are shown in Table 1. Simulation parameters used: $D = 1.76 \times 10^{-5}$ cm^2/s; radius of tip = 5 μm, $i_{T,\infty} = 1.3$ nA. Scan rate = 0.001 V/s.

Table 1. Kinetic Parameters for Oxidation of Ru(bpy) at Pt Tip UME from SECM Steady-State Voltammograms

no.	$\Delta E_{1/4}$, mV	$\Delta E_{3/4}$, mV	L	i_T	$k°$,[a] cm/s	α	$k°/(D/d)$
1	32	38	0.14	6.1	0.8	0.25	3.1
2	33	42	0.13	6.9	0.8	0.25	3.0
3	34	55	0.12	7.3	0.7	0.32	2.4
4	36	47	0.11	7.7	0.6	0.27	2.0
5	41	69	0.09	10	0.5	0.30	1.2

[a] The fitting for the rate constant was within about ±0.1 cm/s.

for the one-electron oxidation and one-electron reduction should be the same under diffusion-controlled conditions, whereas, in fact, the reduction current was about 20% larger. This can be caused by several factors. The most likely is a perturbation from the presence of a close second reduction wave. To take account of the second reduction wave in the simulation, two CVs (CV1 and CV2) spaced 0.2 V apart (which is close to the experimentally measured difference between the half-wave potentials of the first and second reduction waves, here $E_{1/2}^{CV2} - E_{1/2}^{CV1} \approx 0.2$ V) were simulated and added to generate the simulated CV, CV1 +CV2 (black curve in Figure 6c). At this spacing the simulated CV1+CV2 still had a slightly lower current than the experimental result, possibly because the actual separation between two reduction waves was slightly smaller. Additional factors contributing to a higher limiting current on reduction would be a higher background current (which did not appear to be the case) or an electrostatic (migrational) component to the current, which is less likely at the concentrations of supporting electrolyte (0.1 M) and reactants (0.38 mM) employed. To extract the rate constant for Ru(bpy) reduction, the fit was made between the normalized simulated result (CV1+CV2, for nernstian behavior, Figure 6c, black curve) and the normalized experimental CV (Figure 6c, pink dotted curve). The normalized experimental result fits well to the normalized simulated result for nernstian behavior (Figure 6c), showing that at this distance, where clear kinetic effects are shown for the oxidation, the reduction is essentially nernstian, i.e., with rate constant ≥3 cm/s. Thus the reduction reaction, measured under the same conditions, is at least 4 times larger than that of the oxidation.

Comparison of Heterogeneous Oxidation and Reduction. The explanation for the difference in heterogeneous rate constants is consistent with the previous suggestion of a distance dependency.[1] A reviewer suggested the possibility of a statistical factor on the reduction, because there are three equivalent bpy groups. The electron is probably not delocalized among the bpy groups,[21] However, the electron hopping among the bpy groups is very fast, estimated as ~47 ps.[22] Thus, following the slower heterogeneous ET from the electrode, the electron density is rapidly distributed among the bpy's, in what can be considered a fast-following reaction. Given that the observed reaction rate is larger than diffusion control under our conditions, modification of the estimate >3 cm/s is probably not necessary.

Another issue is whether one can justify the rate difference in terms of the usual Marcus theory factors, such as the reorganization energy, λ. However, even a rough estimate is difficult for a system where one is comparing two moieties within the same molecule, e.g., solvation of the Ru(II) center vs the bpy ligands. This has been done assuming a Born model,[23] for example, but would be difficult for the system under consideration.

The observed difference between the rates of ET for oxidation and reduction on the same molecule and obtained at the same time under the same conditions is thus ascribed to a very simple concept that the bpy ligands act as a barrier for ET to the Ru(II) center. Oxidation via the ligands cannot occur, because the oxidation of the bpy ligands occurs at significantly more positive potentials.[24] Reduction of the exposed ligands occurs with the possibility of a closer approach of the acceptor group to the electrode. The blocking effects of ligands have been observed in the study of photoinduced ET reaction between ruthenium bpy complexes and methyl viologen, where the bpy's were substituted

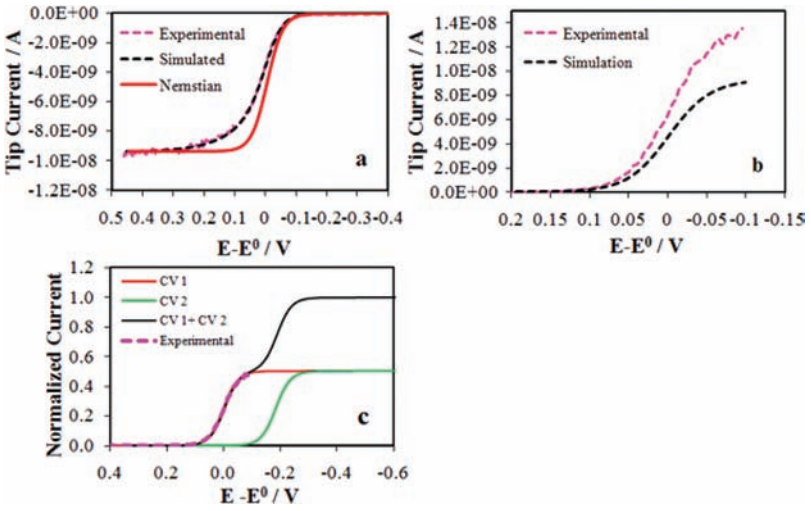

Figure 6. Determination of tip kinetic parameters for Ru(bpy) reduction. (a) Experimental and simulated results for Ru(bpy) oxidation compared to simulated nernstian behavior. (b) Experimental and simulated results for Ru(bpy) reduction. (c) Normalized experimental result and simulated result for the first two waves (CV1+CV2), assumed nernstian with $E_{1/2}^{CV2} - E_{1/2}^{CV1} = 0.2$ V. The solution contained 0.38 mM Ru(bpy) in MeCN with 0.1 M $TBAPF_6$ as supporting electrolyte. Tip−substrate distance was 0.6 μm. Simulation parameters used for both oxidation (panel a) and reduction (panel b): $D = 1.76 \times 10^{-5}$ cm^2/s, radius of tip = 5 μm, $i_{T,\infty} = 1.3$ nA. For panel a, the values obtained from the simulation are $k°/(D/d) = 2$, $k° = 0.6$ cm/s, and $\alpha = 0.3$. For panels b and c, the obtained values are $k° \geq 3$ cm/s and $\alpha = 0.5$. Scan rate = 0.005 V/s.

with propyl, hexyl, or adamantyl groups.[25] The rate constant of the ET reaction decreased with increasing size of the alkyl substituent. Since the other factors in the treatment of ET via Marcus theory were essentially the same, the authors ascribed this trend to the fact that a "bulky substituent decreases the orbital overlap between donor and acceptor", i.e., between the Ru(bpy) (D) and MV^{2+} (A), and treated this by a tunneling effect (the electronic coupling matrix elements, H_{rp}).[25] Although the ET here involves oxidation of the Ru(II) center, it demonstrates the importance of distance effects in ET rates with Ru(bpy) complexes. These findings encouraged us to estimate how the difference in rate relates to the difference in ET distance and the β value in eq 1. The distance from the Ru center to the H atom para to the N on the pyridine ring is 4.746 Å, from the bond distances and bond angles reported by Rillema et al.[26] The approach of the molecule to an electrode may be slightly smaller, so we take a distance, x, of 4 Å. From the minimum difference between the rate constant for oxidation, 0.7 cm/s, and that for reduction, 3 cm/s, a β value of 0.4 Å^{-1} is found. This number is smaller than expected for transfer through an alkyl chain, where $\beta \approx 1$ Å^{-1}. This suggests that either the actual reduction rate constant is considerably larger, e.g., 20−30 cm/s, or the bpy ligands can behave as conjugated spacers.[4,5]

CONCLUSIONS

Oxidation and reduction of a donor−acceptor molecule, $Ru(bpy)_3^{2+}$, with Ru as the donor in the center, connected to three 2,2′-bipyridine ligands as acceptors, have different heterogeneous electron-transfer kinetics. The rate constants for Ru(bpy) oxidation and reduction in nonaqueous solvent (acetonitrile) and an inert atmosphere were successfully measured using SECM with a Pt ultramicroelectrode held in close proximity to a conductive substrate, where the mass-transfer rate is relatively large compared to the electron-transfer rate. The results show that the steady-state voltammogram for Ru(bpy) oxidation deviates from nernstian behavior, while Ru(bpy) reduction is essentially nernstian, with a rate constant at least 4 times larger than that of oxidation. Differences in the rates of heterogeneous ET from the buried Ru(II) center to the more available bpy ligand suggest that tunneling effects may be important. Assuming other factors influencing the rates of Ru(bpy) oxidation and reduction are the same, a tunneling constant (β value) of 0.4 Å^{-1} was calculated. SECM is a useful technique to study heterogeneous ET of different moieties of the same molecule under identical experimental conditions. It will be interesting to extend this study to other D−A molecules with different distances for ET to see if tunneling effects can provide a guide to the relative rates of electron transfer.

AUTHOR INFORMATION

Corresponding Author
ajbard@mail.utexas.edu

ACKNOWLEDGMENT

We thank the National Science Foundation (CHE 0808927) and the Robert A. Welch Foundation (F-0021) for financial support of this research and Joaquin Rodriguez-Lopez for helpful discussions, as well as the Microscopy and Imaging Facility of the Institute for Cellular and Molecular Biology at The University of Texas at Austin for SEM.

REFERENCES

(1) Shen, M.; Rodríguez-López, J.; Huang, J.; Liu, Q.; Zhu, X.-H.; Bard, A. J. *J. Am. Chem. Soc.* **2010**, *132*, 13453–13461.
(2) Finklea, H. O. In *Electroanalytical Chemistry*; Bard, A. J., Rubinstein, I., Eds.; Marcel Dekker: New York, 1996; Vol. 19, pp 109–135.
(3) Smalley, J. F.; Feldberg, S. W.; Chidsey, C. E. D.; Linford, M. R.; Newton, M. D.; Liu, Y.-P. *J. Phys. Chem.* **1995**, *99*, 13141–13149.
(4) Sachs, S. B.; Dudek, S. P.; Hsung, R. P.; Sita, L. R.; Smalley, J. F.; Newton, M. D.; Feldberg, S. W.; Chidsey, C. E. D. *J. Am. Chem. Soc.* **1997**, *119*, 10563–10564.

(5) Creager, S.; Yu, S. J.; Bamdad, D.; O'Conner, S.; MacLean, T.; Lam, E.; Chong, Y.; Olsen, G. T.; Luo, J.; Gozin, M.; Kayyem, J. F. *J. Am. Chem. Soc.* **1999**, *121*, 1059–1064.
(6) Juris, A.; Balzani, V.; Barigelletti, F.; Campagna, S.; Belser, P.; Von Zelewsky, A. *Coord. Chem. Rev.* **1988**, *84*, 85–277.
(7) Sun, P.; Mirkin, M. V. *Anal. Chem.* **2006**, *78*, 6526–6534.
(8) Zhou, J. F.; Zu, Y. B.; Bard, A. J. *J. Electroanal. Chem.* **2000**, *491*, 22–29.
(9) Mirkin, M. V.; Bard, A. J. *Anal. Chem.* **1992**, *64*, 2293–2302.
(10) Mirkin, M. V.; Bulhões, L. O. S.; Bard, A. J. *J. Am. Chem. Soc.* **1993**, *115*, 201–204.
(11) Ding, Z. F.; Quinn, B. M.; Bard, A. J. *J. Phys. Chem. B* **2001**, *105*, 6367–6374.
(12) Bard, A. J.; Mirkin, M. V.; Unwin, P. R.; Wipf, D. O. *J. Phys. Chem.* **1992**, *96*, 1861–1868.
(13) *Scanning Electrochemical Microscopy*; Bard, A. J., Mirkin, M. V., Eds.; Marcel Dekker: New York, 2001.
(14) Bard, A. J.; Fan, F.-R. F.; Mirkin, M. V. Scanning Electrochemical Microscopy. In *Electroanalytical Chemistry*; Bard, A. J., Ed.; Marcel Dekker: New York, 1993; Vol. 18, pp 243−373.
(15) Shen, M.; Arroyo-Curras, N.; Bard, A. J. *Anal. Chem.* **2011**, submitted.
(16) Mirkin, M. V.; Richards, T. C.; Bard, A. J. *J. Phys. Chem.* **1993**, *97*, 7672–7677.
(17) Mirkin, M. V.; Bard, A. J. *Anal. Chem.* **1993**, *97*, 7672–7677.
(18) Mirkin, M. V.; Bard, A. J. *J. Electrochem. Soc.* **1992**, *139*, 3535–3539.
(19) Rodríguez-López, J.; Minguzzi, A.; Bard, A. J. *J. Phys. Chem. C* **2010**, *114*, 18645–18655.
(20) Wipf, D. O.; Kristensen, E. W.; Deakin, M. R.; Wightman, R. M. *Anal. Chem.* **1988**, *60*, 306–310.
(21) (a) DeArmond, M. K.; Myrick, M. L. *Acc. Chem. Res.* **1989**, *22*, 364–370. (b) Kober, E. M.; Sullivan, B. P.; Meyer, T. J. *Inorg. Chem.* **1984**, *23*, 2098–2104.
(22) Malone, R. A.; Kelley, D. F. *J. Chem. Phys.* **1991**, *95*, 8970–8976.
(23) Amatore, C.; Pflüger, F. *Organometallics* **1999**, *9*, 2276–2282.
(24) (a) Gaudiello, J. G.; Sharp, P. R.; Bard, A. J. *J. Am. Chem. Soc.* **1982**, *104*, 6367–6377. (b) Gaudiello, J. G.; Bradley, P. G.; Norton, K. A.; Woodruff, W. H.; Bard, A. J. *Inorg. Chem.* **1984**, *23*, 3–10.
(25) Hamada, T.; Tanaka, S.; Koga, H.; Sakai, Y.; Sakaki, S. *Dalton Trans.* **2003**, 692–698.
(26) Rillema, D. P.; Jones, D. S.; Woods, C.; Levy, H. A. *Inorg. Chem.* **1992**, *31*, 2935–2938.